Polyethylenimine-Impregnated Resin for High CO_2 Adsorption: An Efficient Adsorbent for CO_2 Capture from Simulated Flue Gas and Ambient Air

Zhenhe Chen,[†] Shubo Deng,*[,†,‡] Haoran Wei,[†] Bin Wang,[†] Jun Huang,[†] and Gang Yu[†,‡]

[†]State Key Joint Laboratory of Environment Simulation and Pollution Control, School of Environment, POPs Research Center, Tsinghua University, Beijing, 100084 China

[‡]Tsinghua University − Veolia Environnement Joint Research Center for Advanced Technology, Tsinghua University, Beijing, 100084 China

ⓢ *Supporting Information*

ABSTRACT: Polyethylenimine (PEI)-impregnated resins with high CO_2 adsorption capacity were successfully prepared in this study. The nonpolar resin HP20 was suitable for PEI loading to achieve high CO_2 adsorption, and the optimal PEI loading was 50 wt %. On the basis of the pore-size distribution of the resin before and after PEI modification, it can be found that mesopores of <43 nm were mainly responsible for PEI loading and pores in the range of 43−68 nm were probably favorable for CO_2 diffusion. The adsorbed amount of CO_2 on HP20/PEI-50 decreased with increasing adsorption temperature because of the dominant role of exothermic reaction of CO_2 adsorption. The adsorption of CO_2 on the adsorbent was very fast, and sorption equilibrium was achieved within 6 min at 75 °C. HP20/PEI-50 almost kept a stable adsorption capacity for CO_2 at concentrations of 15 vol % and 400 ppm in the consecutive adsorption−desorption cycles, and its adsorption capacity was 181 mg/g from pure CO_2 and 99.3 mg/g from 400 ppm CO_2 at 25 °C, higher than all PEI-modified materials reported. The high volume-based amount of CO_2 adsorbed on HP20/PEI-50 (96.0 mg/cm³ at 25 °C and 84.5 mg/cm³ at 75 °C for pure CO_2) is beneficial to reducing the required volume of the adsorption bed for CO_2 capture. This spherical and stable HP20/PEI-50 adsorbent with high and fast CO_2 adsorption exhibits a very promising application in CO_2 capture from flue gas and ambient air.

Appropriate PEI distribution in macroporous resin HP20

KEYWORDS: *CO_2 adsorption, amine-modified adsorbent, carbon capture, polyethylenimine, resin*
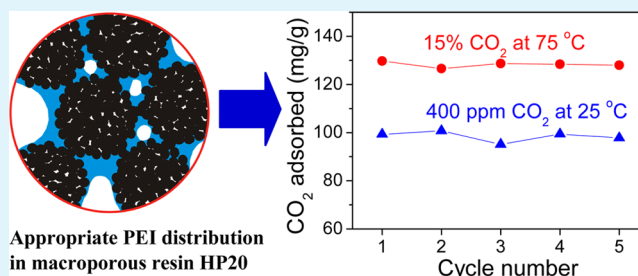
1. INTRODUCTION

In recent years, extensive researches have been focused on CO_2 adsorption on various adsorbents such as activated carbons, zeolite, metal−organic frameworks (MOFs), layered double hydroxides, metal oxide (CaO), and amine-modified materials (AMMs).[1−3] Among the AMMs, polyethylenimine (PEI)-modified porous materials exhibit high CO_2 adsorption at low partial pressure and high selectivity, thermal stability, and regenerability.[4−6] Therefore, the PEI-modified porous materials are excellent candidates for CO_2 capture.

Song et al. developed the "molecular basket" adsorbents by loading PEI into MCM-41, which popularized the PEI-modified adsorbents for CO_2 capture.[7] Both PEI molecular weight and porous materials affect CO_2 adsorption on the PEI-modified adsorbents. Generally, PEI with large molecular weight is stable under high temperature and vacuum conditions, but it is proved that the CO_2 adsorbed amount is negatively associated with the PEI molecular weight due to poor CO_2 diffusion within sticky PEI with high molecular weight.[8−10] Therefore, PEI molecules with number-average molecular weights (M_n) of 600 and 423 were used most frequently.[1] Of course, PEI molecules are easily oxidized in ambient air, but that can be alleviated in the

presence of water.[5,7,11] PEI would also leach under humidity, especially those with small molecular weights.[12] Mesoporous silica materials have attracted much attention because of their versatile pore characteristics and good CO_2 adsorption. The influences of the pore size, pore length, and pore volume of porous materials on CO_2 adsorption have been studied extensively.[13−16] The studies about mesoporous silica support provide us a rough contour of the pore structure of an efficient material for CO_2 adsorption. However, most PEI-modified mesoporous silica materials are fine powders that would have the drawbacks of gradual loss under gas flow, high pressure drop, and corresponding high energy and equipment cost.[17,18] Several researches have focused on the preparation of monolithic adsorbents,[19,20] but the complicated and high cost of mesoporous silica would limit their application in CO_2 capture. Other porous materials have also been used as a PEI support, such as mesoporous alumina[21,22] and carbon black.[23,24] Because of the poor pore properties, the CO_2

adsorbed amount was in the range of 88−154 mg/g, lower than that of most mesoporous silica materials.[21−24]

Adsorptive resins are inborn with spherical shape and thermal stability (temperature below 130 °C). Especially, they have adjustable pores and thus should be a promising porous support to load PEI for CO_2 adsorption. In the literature, only poly(methyl methacrylate) (PMMA)-based resins have been used as supports to load amine-containing chemicals for CO_2 adsorption, such as tetraethylenepentamine-modified PMMA[25] and PEI-modified PMMA,[26] but they have low CO_2 adsorption and poor regeneration. Alesi and Kitchin have also reported the use of an amine-modified ion-exchange resin for carbon capture from 10% CO_2, and the CO_2 adsorbed amounts decrease from 81.4 to 50.6 mg/g when the adsorption temperature increases from 30 to 70 °C.[27] Other resins with suitable pore structure for PEI loading have not been evaluated, and the relationship between the resin properties and PEI loading as well as the adsorption behavior of CO_2 on the PEI-impregnated resins is not clear.

The objective of this study is to develop a PEI-modified resin with fast and high CO_2 adsorption, and we screened and optimized suitable resins for PEI loading, characterized the optimal PEI-modified resin, and evaluated its adsorption behavior for CO_2 under different conditions. The loaded PEI in the hydrophobic resin HP20 was found to be more effective for CO_2 diffusion and adsorption, and the PEI distribution in the resin was also proposed to elucidate the effect of the temperature. Finally, CO_2 adsorption on the PEI-modified resin from 15% CO_2 and 400 ppm CO_2 in N_2 was performed to evaluate its possibility for CO_2 capture from flue gas and ambient air.

2. MATERIALS AND METHODS

2.1. Chemicals and Materials. PEI with M_n of 600 and a density of 1.03 g/cm^3 was purchased from Alfa Aesar Company. The commercial resins, including XAD4, XAD7HP, HP2MG, and HP20, were purchased from Sigma-Aldrich Company. The resins D4020 and DA201 were provided by Chemical Plant of Nankai University and Tianjin Haiguang Chemical Company, Ltd., respectively. The properties of these resins are listed in Table S1 in the Supporting Information.

2.2. Preparation of PEI-Impregnated Resins. The six resins were first sieved to collect fractions in the range of 35−60 mesh (0.25−0.43 mm) for PEI loading, and then the resins were dried at 105 °C for 12 h to remove the adsorbed water until no weight loss was observed. The PEI-modified resins were prepared by a wet impregnation method with slight modification.[5−9] The predetermined amount of PEI was dissolved in 2.75 mL of methanol under stirring for 15 min, and then 0.5 g of resin was added into the solution. The mixture was continuously stirred at 150 rpm for 12 h and then dried at 70 °C for 12 h under a vacuum of 700 mmHg in a rotary vacuum evaporator. The obtained PEI-impregnated resins are denoted as Resin/PEI-*X*, where *X* represents the weight percentage of PEI in the PEI-impregnated resins.

2.3. Adsorbent Characterization. The resin HP20 before and after PEI loading was characterized by N_2 adsorption at 77 K in a gas adsorption instrument (Autosorb iQ, Quantachrome Corp., Boynton Beach, FL). Prior to the measurements, the resin samples were outgassed for 4 h in the degas pot of the adsorption instrument at 50 °C.[28] Their specific surface areas were determined by the Brunauer−Emmett−Teller (BET) method and were calculated from the adsorption data in the relative pressure intervals from 0.01 to 0.2, and the total pore volume was determined from the adsorbed amount at a relative pressure of about 0.99. The pore-size distribution was obtained according to the nonlocal density functional theory.

2.4. CO_2 Adsorption from Pure and 15% CO_2. CO_2 adsorption from pure CO_2 at 1 bar was measured with a thermogravimetric analyzer (Mettler Toledo). The weight change of the adsorbent was recorded to determine the adsorption of CO_2 on the materials. In a typical adsorption process, 10 mg of the adsorbent was placed in a small sample cell, then heated to 100 °C in a N_2 atmosphere at a flow of 60 mL/min, and held at that temperature (about 30 min) until no weight loss was observed. The temperature was then adjusted to the desired temperature and held for 20 min to stabilize the sample weight and temperature. Finally, ultrapure CO_2 was introduced at a flow rate of 60 mL/min for 60 min.

Consecutive CO_2 adsorption from 15 vol % CO_2 (N_2 as the balance gas) and desorption were also conducted on the thermogravimetric analyzer. All of the parameters were the same as those for adsorption from pure CO_2 except for the temperature of 75 °C and 15 vol % CO_2. After 1 h of adsorption, the testing gas was switched to pure N_2 at a flow rate of 60 mL/min and the temperature was raised to 100 °C at a heating rate of 10 °C/min to perform desorption of CO_2. The desorption time was 30 min, and the temperature was then adjusted to 75 °C and stabilized for 20 min before the next adsorption. Five adsorption−desorption cycles were conducted.

2.5. CO_2 Adsorption from 400 ppm CO_2. CO_2 adsorption from 400 ppm CO_2 (N_2 as the balance gas) was performed with a self-made system, similar to that in the literature.[8,29] Briefly, the system contains a U-shaped glass tube capped with a septum and connected to the gas-delivery system via needles inserted through the septum. The gas-delivery system includes a regeneration gas (ultrapure N_2) and an adsorption gas (400 ppm CO_2) controlled by two volumetric flowmeters. The adsorption and regeneration temperatures were controlled by an oil bath. For a typical adsorption process, about 0.5 g of HP20/PEI-50 was loaded into the U-shaped glass tube and a layer of glass wool placed over it to stabilize the adsorbent bed. HP20/PEI-50 was pretreated by heating at 100 °C in the oil bath under the protection of ultrapure N_2 with a flow rate of 100 mL/min for 3 h to desorb CO_2 and water from the adsorbent. HP20/PEI-50 was then cooled to 25 °C to measure the weight of the tube, followed by the introduction of 400 ppm CO_2. After adsorption for 12 h at atmospheric pressure, the weight of the glass tube was measured again. The adsorbed amount (CO_2 and H_2O) on HP20/PEI-50 was determined by the weight difference of the glass tube before and after CO_2 adsorption. To eliminate the influence of adsorbed water, a control adsorption experiment from ultrapure N_2 with the same humid content as that of 400 ppm CO_2 was also conducted, and the obtained weight of adsorbed water was deducted from the adsorbed amount (CO_2 and H_2O) from 400 ppm CO_2 to achieve the CO_2 adsorbed amount. Because both ultrapure N_2 and 400 ppm CO_2 used in this study contained water of less than 3 ppm, the adsorbed water and enhanced CO_2 adsorbed amount due to the presence of water on the adsorbent in the whole adsorption process were negligible (<0.8%). Desorption was performed with the same procedure as the pretreatment of adsorbent and then cooled to 25 °C, followed by measurement of the adsorbent weight again for the next adsorption cycle. Five adsorption−desorption cycles were conducted to evaluate the adsorbent regeneration.

3. RESULTS AND DISCUSSION

3.1. CO_2 Adsorption on Different PEI-Impregnated Resins. Several commercially available resins with different pore sizes and surface polarities were selected to load PEI. HP2MG and XAD7 are composed of polymethacrylate, DA201 is composed of poly(styrene−cyanoethylene), and other resins consist of polystyrene (Table S1 in the Supporting Information). All pristine resins look creamy white after water removal at 105 °C, while the dried resins with 40 wt % PEI exhibit different transparencies. The modified XAD4 and D4020 are transparent, the modified XAD7 exhibits partially transparent, and other resins are creamy white. The transparency indicates a loss of discontinuities or porous structure

after PEI loading, unfavorable for CO_2 adsorption because of the difficult diffusion of CO_2 to the inner amine groups. The creamy white of PEI-modified DA201, HP2MG, and HP20 indicates that that some pores are still available after PEI loading.

The adsorbed amounts of CO_2 on the PEI-modified resins follow the decreasing order of HP20 > DA201 > HP2MG > XAD7HP > NKA > XAD4 > D4020 (Figure 1). XAD4 and
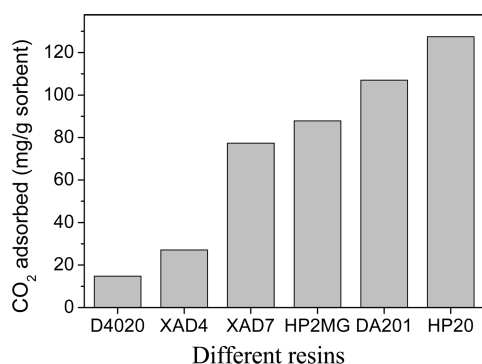

Figure 1. Pure CO_2 adsorption at 75 °C and 1 bar on the different resins containing 40 wt % PEI.

D4020 with the smallest pore size of around 10 nm have the lowest adsorption capacity, indicating that resins with small pore size are not suitable for PEI loading. It is clear that the creamy-white PEI-modified resins (HP20, DA201, and HP2MG) have higher CO_2 adsorbed amounts than others because of the presence of unoccupied pores for easy CO_2 diffusion. HP2MG and HP20 are similar to each other in pore size, pore volume, and surface area, but the amount of CO_2 adsorbed on HP20/PEI-40 is much higher than that on HP2MG/PEI-40. Perhaps, the nonpolar surface of hydrophobic HP20 is unfavorable for the close attachment of hydrophilic PEI. When the resin pores are impregnated by excess PEI molecules, CO_2 may easily diffuse into the pores via the gaps between the resin surface and PEI, making more PEI molecules available for CO_2 adsorption. Because the pore volume of HP20 is higher than that of DA201, the theoretical maximum PEI (M_n = 600) loading in HP20 (57.2 wt %) is higher than that in DA201 (45.2 wt %). Evidently, both the pore properties and matrix hydrophobicity affect CO_2 adsorption on the PEI-impreganted resins. In view of the highest CO_2 adsorbed amount on HP20/PEI-40 and the potential more PEI loading for CO_2 adsorption, HP20 was selected to further optimize preparation of the PEI-modified adsorbent.

3.2. Effect of PEI Loading on CO_2 Adsorption. The influence of the PEI content in the HP20/PEI adsorbents on CO_2 adsorption at 75 °C (typical flue gas temperature) and 25 °C (typical air temperature) is shown in Figure 2. The CO_2 adsorbed amount at 25 °C is higher than that at 75 °C. They all linearly increase first and then decrease rapidly with increasing PEI content, and the maximum CO_2 adsorption (159.6 mg/g at 75 °C and 181 mg/g at 25 °C) is achieved when the adsorbent contains 50 wt % PEI (Figure 2a). Because the maximum theoretical PEI loading in HP20 is 57.2 wt %, the best PEI loading of 50 wt % indicates that some remaining pores are necessary to ensure the easy diffusion of CO_2 in the adsorbent.

PEI in the adsorbent is the active ingredient for CO_2 adsorption, and the amine efficiency (CO_2 adsorbed amount based on per mmol of N in PEI) is presented in Figure 2b,
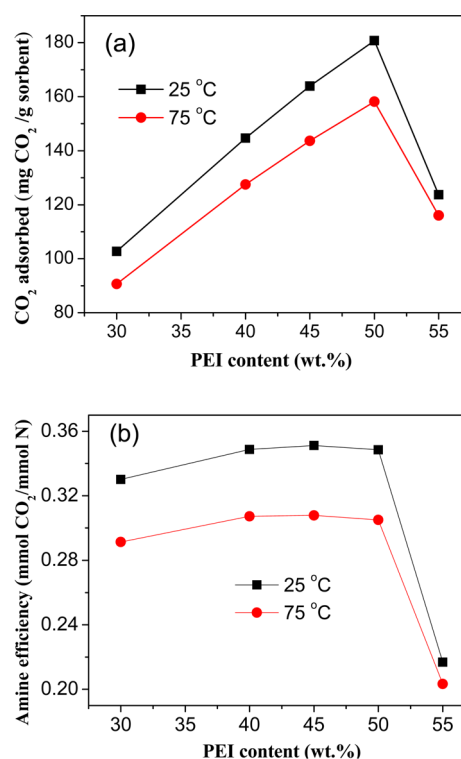

Figure 2. Effect of the PEI content on pure CO_2 (1 bar) adsorption on PEI-impregnated HP20: (a) adsorbed amount expressed by the unit of mg of CO_2/g of adsorbent; (b) amine efficiency expressed by the unit of mmol of CO_2/mmol of N.

assuming that PEI possesses a N_2 content of about 33% by weight.[10,12] The amine efficiency is about 0.35 mmol of CO_2/mmol of N in the PEI content range of 40−50%, close to the theoretical value of 0.39 mmol of CO_2/mmol of N.[12] The amine efficiency remained relatively stable in the PEI range of 30−50% and decreased significantly with further increasing PEI content, indicating that the low amount of loaded PEI in the resin was more efficient for CO_2 adsorption because of the more available amine groups in the loaded PEI molecules. The gradually increasing CO_2 adsorption with increasing PEI content from 30% to 45% may be related to more PEI molecules available for CO_2 adsorption at higher PEI content after a certain number of PEI molecules were loaded in the micropores, which are ineffective for CO_2 adsorption.

3.3. Textural Characterization of the PEI-Impregnated HP20. Textural characteristics such as the pore size, pore volume, and surface area may be related to CO_2 adsorption on the PEI-modified adsorbent. As shown in Table S2 in the Supporting Information, the BET surface area and pore volume of PEI-impregnated HP20 both decrease with increasing PEI concentrations. The pore volume and surface area are closely related to the amount of PEI loaded in the resin, and more loaded PEI indicated the lower pore volume and surface area of the modified adsorbent. In consideration of the CO_2 adsorbed amount (Figure 2a), the pore volume and surface area of PEI-modified HP20 have no direct correlation with CO_2 adsorption. The difference between the pore volume lost and the loaded PEI volume is shown in Table S2 in the Supporting Information. A negative value of this parameter (Δ volume) suggests that some PEI molecules were not loaded into the resin, while a positive value suggests that some pores were blocked by PEI and inaccessible to N_2 adsorption.[31] For HP20/

PEI-30, the positive Δ volume indicates that PEI may not diffuse into some small pores and just block their entrances. For the adsorbents with PEI loading from 40 to 55wt %, the Δ volume values are negative and stable (-0.08 to -0.09 cm^3/g), suggesting that a fixed amount of PEI was not loaded into the resin because of the limitation of the wet-impregnation method.

The pore-size distribution of PEI-modified HP20 could give information for the PEI location inside the porous resin. The pore-size distribution of HP20 before and after PEI loading is illustrated in Figure 3, calculated from the N$_2$ adsorption—
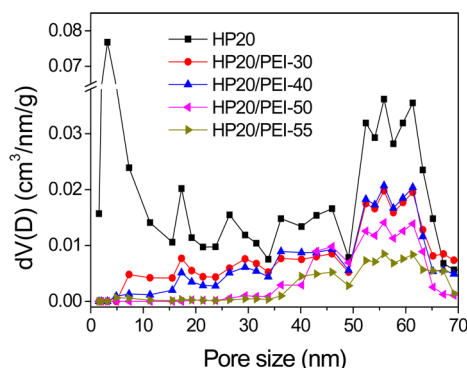

Figure 3. Pore-size distribution of HP20 before and after PEI loading.

desorption isotherm (Figure S1 in the Supporting Information). HP20 contains main mesopores and macropores as well as a few micropores (volume = 0.025 cm^3/g). Microspheres are the microscopic units of resin HP20 based on the styrene—divinylbenzene network; mesopores are mainly the interstices between the microspheres, and macropores are mainly the spaces between the agglomerates of the microspheres.[31,32] Agglomerates of particles with various sizes inside the porous copolymer are responsible for the wide pore-size distribution of HP20.[32] In general, PEI molecules prefer to load in small pores in a porous material with multiple types of pores because the surface potential of small pores is higher than that of large pores. For HP20/PEI-30, the pore volume decreases in the whole size range, especially at pore sizes below 10 nm (Figure 3), indicating that these pores were blocked by PEI and inaccessible to N$_2$ adsorption. With further increasing PEI concentrations, the pores below 35 nm are gradually filled with PEI, and these pores almost disappear for HP20/PEI-50. The pores above 35 nm especially in the range of 50–68 nm are available for HP20/PEI-50, and they decrease significantly in HP20/PEI-55, indicating that PEI is prone to first filling small pores and then large pores; namely, PEI is not uniformly distributed in the resin. Because HP20/PEI-50 has the highest CO$_2$ adsorbed amount, the pores in the size range of 43–68 nm may be favorable for CO$_2$ diffusion into the resin during the adsorption process, exposing more active surfaces for CO$_2$ uptake. When these pores are overloaded with PEI, CO$_2$ is difficult to diffuse into the resin and adsorb on the loaded PEI. Therefore, the appropriate amount of PEI should be loaded in the resin, and some pores should be available for CO$_2$ diffusion into the porous material.

On the basis of the above results, we proposed the PEI distribution in HP20. HP20 is composed of microspheres (Figure 4a), and one microsphere (about 100 nm) also consists of many nuclei (about 10 nm); the micropores of <2 nm are formed between nuclei.[32] The micropore volume of HP20 is only 0.025 cm^3/g calculated from N$_2$ adsorption, which implies
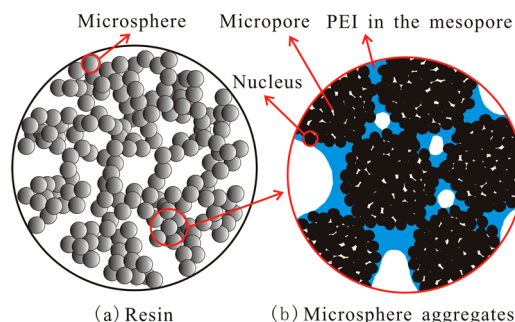

Figure 4. Schematic diagram for PEI distribution in HP20.

less PEI loading in micropores. Moreover, the 3D size of a single PEI molecule is 1.4 nm × 1.0 nm × 0.6 nm (estimated by Chemoffice, CambridgeSoft), which is difficult to diffuse into these micropores. Consequently, PEI molecules are mainly loaded on the surface of microspheres. By contrast, mesopores in the range of 2–43 nm decrease gradually with increasing PEI loading (Figure 3), indicating that PEI molecules mainly locate in the mesopores between microspheres (Figure 4b). Meanwhile, a fraction of PEI could also locate in the mesopores on the surface of the microspheres (Figure 4b).

The interstice between microspheres is in the shape of a hoop and connected with others, which means less diffusion resistance and a faster adsorption of CO$_2$ than the PEI-modified mesoporous silica such as MCM-41 and SBA-15, in which CO$_2$ could only approach the loaded PEI from the two ends of the cylindrical pores.[9,33] The big pores in the range of 43–68 nm shown in Figure 4b can serve as pathways for CO$_2$ diffusion. The overloading of PEI in the resin would block these big pores, and CO$_2$ is difficult to diffuse into the bulky and sticky PEI phase. Therefore, the loading of 50 wt % PEI in HP20 is appropriate to maintain the porous structure and high CO$_2$ adsorption. According to the pore volume of HP20/PEI-50 and HP20 in Table S2 in the Supporting Information, it can be calculated that about 58% of the volume of the resin HP20 was occupied by PEI.

3.4. Effect of the Temperature on CO$_2$ Adsorption. CO$_2$ adsorption on HP20/PEI-50 at temperatures ranging from 25 to 90 °C is shown in Figure 5. The amount of CO$_2$ adsorbed on the adsorbent decreased with increasing temperature, and the CO$_2$ adsorbed amount was 181 mg/g at 25 °C and decreased to 141 mg/g at 90 °C, indicating that high temperature is not favorable for CO$_2$ adsorption on HP20/PEI-50. Usually, the adsorption temperature has two different

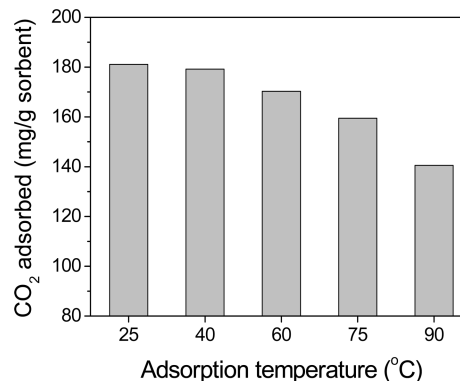**Figure 5.** CO$_2$ adsorption at different temperatures on HP20/PEI-50.

effects on CO_2 adsorption on the PEI-modified materials. On the one hand, increasing temperature is disadvantageous to CO_2 adsorption on the PEI-modified materials because of the exothermic reaction.[33] On the other hand, enhanced temperature is favorable for CO_2 adsorption because CO_2 molecules more easily diffuse into the PEI phase to contact more amine groups in PEI at higher temperature.[34] The decrease of CO_2 adsorption on HP20/PEI-50 with increasing temperature indicates the dominant effect of the exothermic reaction. It has been reported that PEI-modified glass fibers also have high CO_2 at low temperature,[35] and the negative effect of the exothermic reaction may be higher than the positive effect of efficient PEI diffusion at higher temperature due to the loading of PEI on the surface of a nonporous fiber. However, CO_2 adsorption on the pore-expanded MCM-41 loaded with 55 wt % PEI,[36] MCM-41 with 50 wt % PEI, and SBA-15 with 50 wt % PEI increases with increasing temperature (below 75 °C),[8,33] indicating that the positive effect of CO_2 diffusion in PEI is dominant. It is interesting that increasing temperature is unfavorable for CO_2 adsorption on SBA-15 loaded with 30 wt % PEI,[37] and the possible reason is that PEI molecules exist in the form of a thin film in the pores, which is easy for CO_2 diffusion. Therefore, increasing temperature is advantageous to CO_2 adsorption only when the porous materials are overloaded with PEI and diffusion resistance of CO_2 is too large to access and react with amine groups in PEI molecules.

3.5. Adsorption Kinetics and Modeling. For CO_2 capture, adsorbents should possess not only a high sorption capacity but also fast adsorption to be energy-efficient. A recent study shows that the overloading of amines on adsorbents can help the equilibrium capacity but harm adsorption kinetics in a dynamic process.[38] Figure 6 illustrates the adsorption kinetics
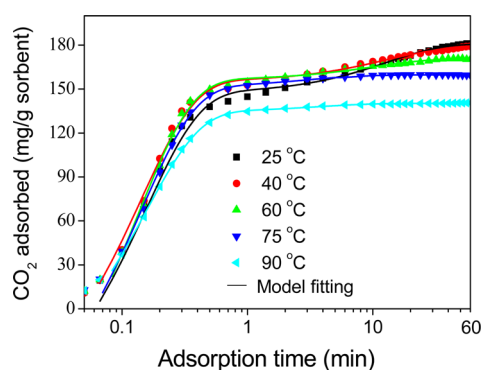

Figure 6. CO_2 adsorption kinetics on HP20/PEI-50 at different temperatures and fittings using the DEM (adsorption time = 60 min).

of CO_2 on HP20/PEI-50 at different temperatures. Generally, the CO_2 adsorption process on the PEI-modified materials contains fast (corresponding amine groups on the surface of

PEI aggregates) and slow adsorption steps (corresponding amine groups buried in PEI aggregates), and fast adsorption of CO_2 on HP20/PEI-50 can be achieved within a few minutes.[29] At 90 and 75 °C, CO_2 adsorption equilibrium was almost reached within about 2 and 6 min, respectively. With a decrease of the adsorption temperature, slow CO_2 adsorption on HP20/PEI-50 becomes obvious. At 25 °C, the slow adsorption step is much more significant and adsorption equilibrium was not achieved at 15 min. It is obvious that CO_2 adsorption on HP20/PEI-50 is slow at low temperature, and it is associated with the strong CO_2 diffusion resistance in the PEI phase at low temperature. The enhanced diffusion of CO_2 in PEI films loaded in the resin becomes obvious at temperatures above 75 °C.

HP20/PEI-50 requires 1 min to reach 95.5% of its CO_2 adsorbed amount at 60 min at 75 °C and 1 min to reach 79.8% at 25 °C. In comparison, the PEI-modified silica required 5 min to reach 87% and 68% of its CO_2 adsorbed amount at 60 min at 75 and 30 °C, respectively.[22] At 70 °C, the PEI-impregnated mesocellular foam took 5 min to reach 84% of the CO_2 adsorbed amount at 60 min, while the value was only 62.5% at 30 °C.[39] Evidently, CO_2 adsorption on HP20/PEI-50 is faster than that of other reported PEI-modified materials, possibly because of the appropriate pores and loose attachment of PEI on the nonpolar resin surface to facilitate CO_2 diffusion.

A double-exponential model (DEM) was applied to describe the adsorption kinetics of CO_2 on HP20/PEI-50. The model is suitable for the adsorbent with two different types of adsorption sites, and the adsorption process contains fast and slow adsorption steps.[40,41] The model can be expressed as follows:

$$q_t = q_e - D_1 \exp(-K_1 t) - D_2 \exp(-K_2 t) \qquad (1)$$

where D_1 (mg/g) and K_1 (min^{-1}) are the adsorption rate and diffusion parameter, respectively, for the fast step and D_2 and K_2 are the adsorption rate and diffusion parameter, respectively, for the slow step. To determine the adequacy of this model, an error function (Err) based on the normalized standard deviation was applied.[42]

$$\text{Err (\%)} = \sqrt{\frac{\sum \left[(q_{t(\exp)} - q_{t(\text{mod})})/q_{t(\exp)}\right]^2}{N - 1}} \times 100 \qquad (2)$$

where $q_{t(\exp)}$ is the adsorbed amount at a given time determined experimentally, $q_{t(\text{mod})}$ is the adsorbed amount predicted by the model, and N is the total number of experimental points.

Table 1 shows the obtained parameters of the DEM model, the correlation coefficient (R^2), and Err. The high R^2 (>99%) and low Err (<1%) indicate the good fitting using this model. The DEM model described the experimental data very well at all of the different temperatures (Figure 6). For the fast adsorption step, both D_1 and K_1 first increase and then decrease with increasing temperature from 25 to 90 °C, and the highest

Table 1. Parameters of the DEM Kinetic Model Obtained for CO_2 Adsorption on HP20/PEI-50

		fast adsorption		slow adsorption			
temperature (°C)	q_e (mg/g)	D_1 (mg/g)	K_1 (min^{-1})	D_2 (mg/g)	K_2 (min^{-1})	Err (%)	R^2
25	180.8	218.7	6.499	33.9	0.077	0.884	0.994
40	178.3	219.9	7.061	23.4	0.080	0.143	0.990
60	170.6	248.3	7.404	14.6	0.097	0.351	0.992
75	159.6	229.1	7.040	8.85	0.321	0.321	0.998
90	140.2	185.5	6.471	6.13	0.266	0.123	0.998

D_1 and K_1 are obtained at 60 °C. For the slow adsorption step, the adsorption rate constant D_2 decreases, while the diffusion rate constant K_2 increases with increasing temperature from 25 to 90 °C, suggesting that some amine groups buried in the PEI film are still active to adsorb CO_2 at low temperature but the high diffusion resistance causes the slow adsorption of CO_2.[20] Evidently, HP20/PEI-50 shows high and fast adsorption for CO_2 at 75 °C, exhibiting a promising application in CO_2 capture from flue gas.

3.6. Consecutive CO_2 Adsorption and Desorption.

CO_2 adsorption from flue gas is one of the most important ways to reduce atmospheric CO_2, which is believed to be the archcriminal of climate change.[43] Typically, flue gas from a postcombustion power plant contains 10−15 vol % CO_2 with temperatures in the range of 50−75 °C.[44] To investigate the possibility of HP20/PEI-50 for CO_2 capture from flue gas, consecutive CO_2 adsorption and desorption on HP20/PEI-50 was conducted five times at 75 °C with a gas stream containing 15 vol % CO_2 and 85 vol % N_2. The CO_2 adsorbed amounts on HP20/PEI-50 remained constant in the five cycles (Figure 7).
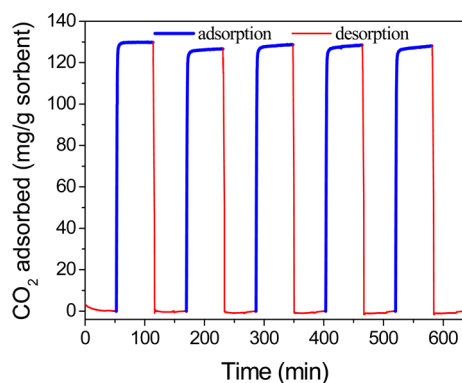

Figure 7. Thermogravimetric analysis curves for five CO_2 adsorption−desorption cycles on HP20/PEI-50 at 75 °C with 15% CO_2 in N_2 (adsorption time = 60 min).

The amount of CO_2 adsorbed was 129.7 mg/g in the first cycle and still reached 128.0 mg/g in the fifth run. Obviously, HP20/PEI-50 possesses high and stable CO_2 adsorption in the adsorption and desorption cycles, and the stable baseline indicates that the adsorbent could be regenerated completely after five cycles. In addition, the presence of humidity in the flue gas may affect CO_2 adsorption on PEI-modified HP20. The adsorption of 15% CO_2 on HP20/PEI-50 at 75 °C under 100% humidity and dry conditions was compared (Figure S2 in the Supporting Information). The CO_2 adsorbed amount increased obviously under humid conditions, which is consistent with other PEI-modified adsorbents.[23,26,30] It is notable that the condensing water may wash the soluble PEI out of the resin in the CO_2 adsorption process for a long time, which needs to be further evaluated in the actual application.

CO_2 capture from ambient air has also been proposed as a means of decreasing the CO_2 level in the atmosphere to combat climate change.[45−48] HP20/PEI-50 has high CO_2 adsorption at 25 °C in pure CO_2, and it should also have a high adsorption capacity for CO_2 in air. When 400 ppm CO_2 in N_2 was adopted to simulate ambient air,[18,49] the adsorbed amounts of CO_2 on HP20/PEI-50 at 25 °C in the five consecutive adsorption cycles are illustrated in Figure 8. The CO_2 adsorbed amounts remained almost stable in the five cycles, and it was 99.3
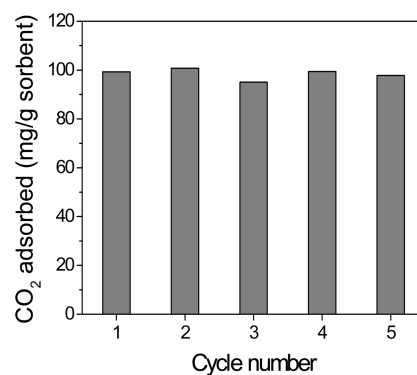

Figure 8. Adsorbed amount of CO_2 on HP20/PEI-50 at 25 °C from 400 ppm CO_2 in N_2 in the five adsorption cycles.

mg/g for the first adsorption and 97.8 mg/g for the fifth run. Additionally, 587.2 mg of HP20/PEI-50 was added in the adsorption bed, and the adsorbent mass was 586.8 mg after five cycles. Almost no loss or weight gain of the adsorbent indicated the stability of HP20/PEI-50 in the CO_2 adsorption process.

Currently, the PEI-based adsorbents are normally regenerated via vacuum swing adsorption (VSA) or heating in a flowing inert gas (nitrogen, argon, etc.) at high temperature on a laboratory scale. However, heating in a flowing inert gas does not produce a concentrated product, and VSA is not scalable for carbon capture from flue gas or ambient air. Jones et al. suggested that water vapor (usually less than 110 °C) could be used to regenerate the PEI-modified adsorbents effectively, considering that steam is sometimes discharged as waste in industrial processes and the presence of water vapor could also avoid the irreversible formation of urea at high temperature and dry conditions.[10,50] Since the resin HP20 can be used at temperature up to 130 °C, it is possible that the HP20/PEI-50 could be regenerated with water vapor without anxiety about the loss of adsorbed amount due to pore collapse as happened on MCM-41, MCF or SBA-15 based adsorbents.[10,50] However, the PEI leaching in the presence of water vapor and the stability of CO_2 adsorption on the HP20/PEI-50 should be evaluated in the following study.

3.7. Comparison of the CO_2 Adsorption Capacity.

Table 2 shows the CO_2 adsorbed amounts on some PEI-modified adsorbents reported in the literature. When pure CO_2 is used to evaluate the adsorption capacity of the PEI-modified adsorbents, the CO_2 adsorbed amounts are in the range of 133−218 mg/g at 75 °C and 33−149 mg/g at 25 °C and 1 bar. Although the amount of CO_2 adsorbed on HP20/PEI-50 at 75 °C is lower than those of a few adsorbents, it is up to 181 mg/g at 25 °C, higher than those of all other PEI-modified adsorbents reported. The PEI-based amount of CO_2 uptake could reflect the PEI efficiency for CO_2 capture and textural advantages of porous materials. As listed in Table 2, the CO_2 adsorbed amounts on the PEI-modified materials are in the range of 237−370 mg/g of PEI at 75 °C and 66−259 mg/g of PEI at 25 °C and 1 bar. HP20/PEI-50 has the CO_2 adsorbed amount of 316 mg/g of PEI at 75 °C and 362 mg/g of PEI at 25 °C and 1 bar. Evidently, HP20/PEI-50 possesses the highest PEI-based CO_2 adsorption at 25 °C and 1 bar among all of the PEI-modified adsorbents, indicating that the more loaded PEI molecules are utilized to adsorb CO_2. A high density of adsorbent is beneficial to reducing the required volume of the adsorption bed for CO_2 capture. The tap density of HP20/PEI-50 was measured to be 0.53 g/cm³, and the CO_2 adsorbed

6942

dx.doi.org/10.1021/am400661b | ACS Appl. Mater. Interfaces 2013, 5, 6937−6945

Table 2. Comparison of HP20/PEI-50 with Other PEI-Modified Adsorbents

| porous material | PEI (M_n) | T (°C) | $P_{CO_2}{}^g$ (bar) | CO$_2$ adsorbed amount | | ref |
				adsorbent-based (mg/g of adsorbent)	PEI-based (mg/g of PEI)^h	
HP20	600	75	1	159.6	316	this study
		75	0.15	129.7	259.4	
		25	1	181	362	
		25	400 ppm	99.3	199	
HMS^a	600	75	1	218	335	20
SBA-15	423	75	1	173	314	15
PMCM-41^b	423	75	1	203	370	36
carbon black	423	75	1	154	237	23
MCM-41	423	75	1	133	266	33
MCF^c	600	70	1	198	330	39
P-silica^d	600	70	1	147	294	8
P-silica	25000	70	1	130	260	8
silica monolith	600	80	1	167	334	55
MCM-41	423	25	1	32.9	66.0	56
carbon black	423	25	1	63.8	128	23
PMCM-41	423	25	1	74.8	136	36
SBA-15	423	25	1	112	204	15
MCF	600	30	1	149	248	39
HMS	600	30	1	142	259	20
MHS^e	423	75	0.2	216	260	57
MCF	423	75	0.15	152	304	58
SBA-15	423	75	0.15	105	210	16
alumina	423	75	0.15	49.8	166	22
SBA-15	600	75	0.12	59.8	120	17
SBA-15	423	75	0.1	128	233	15
TMS^f	600	25	400 ppm	96.4	212	51
fumed silica	25000	25	400 ppm	74.8	150	18
MCF	600	25	400 ppm	46.2	100	49
SBA-15	600	25	400 ppm	46.2	116	21
alumina	600	25	400 ppm	76.6	153	21

^{a}Hierarchical mesoporous silica. ^{b}Pore-enlarged MCM-41 spheres. ^{c}Mesocellular silica foams. ^{d}Precipitated silica. ^{e}Mesoporous hollow silica. ^{f}Tetrapropyl orthotitanate modified mesoporous silica (CARiACT G10). ^{g}CO$_2$ partial pressure. ^{h}CO$_2$ adsorbed amount (mg/g of PEI) = CO$_2$ adsorbed amount (mg/g of adsorbent) × PEI loading amount (wt %).

amount is thus 84.6 mg/cm^3 adsorbent at 75 °C, higher than 47 mg/cm^3 for carbon black loaded with 50 wt % PEI,[23] 70 mg/cm^3 for alumina with a loading of 30 wt % PEI,[22] and 82 mg/cm^3 for precipitated silica loaded with 66.7 wt % PEI.[8] At 25 °C, the CO$_2$ adsorbed amount on HP20/PEI-50 increases to 96.0 mg/cm^3 adsorbent. The high volume-based CO$_2$ adsorption capacity of HP20/PEI-50 is favorable for the actual application in CO$_2$ capture.

Many studies also concentrated on the removal of CO$_2$ from simulated flue gas or ambient air. When the CO$_2$ concentration is 15%, the CO$_2$ adsorbed amounts on the PEI-modified materials are in the range of 59.8–152 mg/g at 75 °C (Table 2), while the value is 129.8 mg/g for HP20/PEI-50. When the adsorption is conducted at a CO$_2$ concentration of 400 ppm, HP20/PEI-50 has a CO$_2$ adsorbed amount of 99.3 mg/g at 25 °C, higher than those of all PEI-modified materials (Table 2). Choi et al. reported the highest CO$_2$ adsorbed amount of 103.8 mg/g after 24 h of adsorption from 390 ppm CO$_2$ at 25 °C, but this adsorbent was not stable and the adsorbed amount decreased to 91.5 mg/g in the second cycle.[51] After modification with tetraethyl orthotitanate, the adsorbed amount is stable around 96.4 mg/g.[51] HP20/PEI-50 also has a higher CO$_2$ adsorption capacity from 400 ppm CO$_2$ at 25 °C than other non-PEI-modified materials reported, such as hyperbranched aminosilica (75.7 mg/g),[52] Mg/DOBDC MOF with

amines (66 mg/g),[53] and alkylamine-appended MOF (88 mg/g),[54] being a very promising candidate for CO$_2$ adsorption from ambient air.

4. CONCLUSIONS

The loading of PEI into the resins is an effective method to preparing novel adsorbents with high CO$_2$ adsorption. The nonpolar resin HP20 impregnated with 50% PEI exhibited fast and high CO$_2$ adsorption at temperatures in the range of 25–90 °C. The efficient PEI molecules loaded in the resins for CO$_2$ adsorption are closely related to the resin porosity and matrix hydrophobicity. The relationship between the resin textural properties and PEI loading as well as the high and fast CO$_2$ adsorption on the PEI-loaded resin was clearly elucidated. On the basis of the size distribution of the resin before and after PEI loading, the pores in the size range of 43–68 nm in HP20/PEI-50 played an important role in CO$_2$ adsorption, resulting in fast CO$_2$ diffusion in the porous materials and the high efficiency of the CO$_2$ reaction with amine groups in PEI molecules. The CO$_2$ adsorption amounts decrease with increasing temperature because of the exothermic reaction of CO$_2$ with amines in PEI. HP20/PEI-50 exhibited a CO$_2$ adsorption capacity of 181 mg/g from pure CO$_2$ and 99.3 mg/g from 400 ppm CO$_2$ at 25 °C, higher than those of other PEI-modified materials. HP20/PEI-50 remained high with an

almost constant CO_2 adsorption capacity under the simulated flue gas at 15% CO_2 and 75 °C as well as the simulated ambient air at 400 ppm CO_2 and 25 °C in the consecutive five adsorption cycles. In general, this novel PEI-impregnated resin had fast and high CO_2 adsorption as well as good reusability, and it is a very competitive and promising adsorbent for carbon capture from both flue gas and ambient air.

ASSOCIATED CONTENT

Ⓢ Supporting Information

Properties of different resins used for PEI impregnation, surface area and pore volume of HP20 before and after PEI loading, N_2 adsorption–desorption isotherms on HP20 before and after PEI loading, and the CO_2 adsorbed amount from 15% CO_2 under 100% humidity. This material is available free of charge via the Internet at http://pubs.acs.org.

AUTHOR INFORMATION

Corresponding Author
*Tel:+ 86 10 62792165. Fax: +86 10 62794006. E-mail: dengshubo@tsinghua.edu.cn.

Notes
The authors declare no competing financial interest.

ACKNOWLEDGMENTS

REFERENCES

(1) Chen, Z. H.; Deng, S. B.; Wei, H. R.; Wang, B.; Huang, J.; Yu, G. *Front. Environ. Sci. Eng.* **2013**, *7*, 326−340.

(2) Samanta, A.; Zhao, A.; Shimizu, G. H.; Sarkar, P.; Gupta, R. *Ind. Eng. Chem. Res.* **2012**, *51*, 1438−1463.

(3) Wei, H. R.; Deng, S. B.; Hu, B. Y.; Chen, Z. H.; Wang, B.; Huang, J.; Yu, G. *ChemSusChem* **2012**, *5*, 2354−2360.

(4) Heydari-Gorji, A.; Sayari, A. *Ind. Eng. Chem. Res.* **2012**, *51*, 6887−6894.

(5) Sayari, A.; Heydari-Gorji, A.; Yang, Y. *J. Am. Chem. Soc.* **2012**, *134*, 13834−13842.

(6) Sayari, A.; Belmabkhout, Y. *J. Am. Chem. Soc.* **2010**, *132*, 6312−6314.

(7) Xu, X.; Song, C.; Andresen, J. M.; Miller, B. G.; Scaroni, A. W. *Microporous Mesoporous Mater.* **2003**, *62*, 29−45.

(8) Goeppert, A.; Meth, S.; Prakash, G. S.; Olah, G. A. *Energy Environ. Sci.* **2010**, *3*, 1949−1960.

(9) Wang, X. X.; Song, C. S. *Catal. Today* **2012**, *194*, 44−52.

(10) Bollini, P.; Didas, S. A.; Jones, C. W. *J. Mater. Chem.* **2011**, *21*, 15100−15120.

(11) Bollini, P.; Choi, S.; Drese, J. H.; Jones, C. W. *Energy Fuels* **2011**, *25*, 2416−2425.

(12) Choi, S.; Drese, J. H.; Jones, C. W. *ChemSusChem* **2009**, *2*, 796−854.

(13) Son, W. J.; Choi, J. S.; Ahn, W. S. *Microporous Mesoporous Mater.* **2008**, *113*, 31−40.

(14) Zelenak, V.; Badanicova, M.; Halamova, D.; Cejka, J.; Zukal, A.; Murafa, N.; Goerigk, G. *Chem. Eng. J.* **2008**, *144*, 336−342.

(15) Heydari-Gorji, A.; Yang, Y.; Sayari, A. *Energy Fuels* **2011**, *25*, 4206−4210.

(16) Yan, X. L.; Zhang, L.; Yan, Z. F.; Yan, G. D.; Yan, Z. F. *Ind. Eng. Chem. Res.* **2011**, *50*, 3220−3226.

(17) Dasgupta, S.; Nanoti, A.; Gupta, P.; Jena, D.; Goswami, A. N.; Garg, M. O. *Sep. Sci. Technol.* **2009**, *44*, 3973−3983.

(18) Goeppert, A.; Czaun, M.; May, R. B.; Prakash, G. S.; Olah, G. A.; Narayanan, S. R. *J. Am. Chem. Soc.* **2011**, *133*, 20164−20167.

(19) Chen, C.; Yang, S. T.; Ahn, W. S.; Ryoo, R. *Chem. Commun.* **2009**, *45*, 3627−3629.

(20) Wang, J. T.; Long, D. H.; Zhou, H. H.; Chen, Q. J.; Liu, X. J.; Ling, L. C. *Energy Environ. Sci.* **2012**, *5*, 5742−5749.

(21) Chaikittisilp, W.; Kim, H. J.; Jones, C. W. *Energy Fuels* **2011**, *25*, 5528−5537.

(22) Yan, X. L.; Zhang, Y.; Qiao, K.; Li, X.; Zhang, Z. Q.; Yan, Z. F.; Komarneni, S. *J. Hazard. Mater.* **2011**, *192*, 1505−1508.

(23) Wang, D. X.; Ma, X. L.; Sentorun-Shalaby, C.; Song, C. S. *Ind. Eng. Chem. Res.* **2012**, *51*, 3048−3057.

(24) Wang, D. X.; Sentorun-Shalaby, C.; Ma, X. L.; Song, C. S. *Energy Fuels* **2011**, *25*, 456−458.

(25) Lee, S.; Filburn, T. P.; Gray, M.; Park, J. W.; Song, H. J. *Ind. Eng. Chem. Res.* **2008**, *47*, 7419−7423.

(26) Gray, M. L.; Hoffman, J. S.; Hreha, D. C.; Fauth, D. J.; Hedges, S. W.; Champagne, K. J.; Pennline, H. W. *Energy Fuels* **2009**, *23*, 4840−4844.

(27) Alesi, W. R.; Kitchin, J. R. *Ind. Eng. Chem. Res.* **2012**, *51*, 6907−6915.

(28) Yue, M. B.; Chun, Y.; Cao, Y.; Dong, X.; Zhu, J. H. *Adv. Funct. Mater.* **2006**, *16*, 1717−1722.

(29) Meth, S.; Goeppert, A.; Prakash, G. K. S.; Olah, G. A. *Energy Fuels* **2012**, *26*, 3082−3090.

(30) Drese, J. H.; Choi, S.; Lively, R. P.; Koros, W. J.; Fauth, D. J.; Gray, M. L.; Jones, C. W. *Adv. Funct. Mater.* **2009**, *19*, 3821−3832.

(31) Sherrington, D. C. *Chem. Commun.* **1998**, *21*, 2275−2286.

(32) Okay, O. *Prog. Polym. Sci.* **2000**, *25*, 711−779.

(33) Xu, X. C.; Song, C. S.; Andresen, J. M.; Miller, B. G.; Scaroni, A. W. *Energy Fuels* **2002**, *16*, 1463−1469.

(34) Kohl, A.; Nielsen, R. *Gas purification*, 5th ed.; Gulf Publishing Co.: Houston, TX, 1997.

(35) Li, P. Y.; Zhang, S. J.; Chen, S. X.; Zhang, Q. K.; Pan, J. J.; Ge, B. Q. *J. Appl. Polym. Sci.* **2008**, *108*, 3851−3858.

(36) Heydari-Gorji, A.; Belmabkhout, Y.; Sayari, A. *Langmuir* **2011**, *27*, 12411−12416.

(37) Kuwahara, Y.; Kang, D. Y.; Copeland, J. R.; Brunelli, N. A.; Didas, S. A.; Bollini, P.; Sievers, C.; Kamegawa, T.; Yamashita, H.; Jones, C. W. *J. Am. Chem. Soc.* **2012**, *134*, 10757−10760.

(38) Bollini, P.; Brunelli, N. A.; Didas, S. A.; Jones, C. W. *Ind. Eng. Chem. Res.* **2012**, *51*, 15153−15162.

(39) Yan, W.; Tang, J.; Bian, Z. J.; Hu, J.; Liu, H. L. *Ind. Eng. Chem. Res.* **2012**, *51*, 3653−3662.

(40) Chiron, N.; Guilet, R.; Deydier, E. *Water Res.* **2003**, *37*, 3079−3086.

(41) Wilczak, A.; Keinath, T. M. *Water Environ. Res.* **1993**, *65*, 238−244.

(42) Serna-Guerrero, R.; Sayari, A. *Chem. Eng. J.* **2010**, *161*, 182−190.

(43) Adegbulugbe, A., Christophersen, Ø., Ishitani, H., Moomaw, W., Moreira, J. In *IPCC Special Report on Carbon Dioxide Capture and Storage*; Davidson, O., de Coninck, H. C., Loos, M., Meyer, L. A., Eds.; Cambridge University Press: Cambridge and New York, 2005; p 51.

(44) D'Alessandro, D. M.; Smit, B.; Long, J. R. *Angew. Chem., Int. Ed.* **2010**, *49*, 6058−6082.

(45) Belmabkhout, Y.; Serna-Guerrero, R.; Sayari, A. *Chem. Eng. Sci.* **2010**, *65*, 3695−3698.

(46) Didas, S. A.; Kulkarni, A. R.; Sholl, D. S.; Jones, C. W. *ChemSusChem* **2012**, *5*, 2058−2064.

(47) Jia, X.; Yan, H.; Wang, Z. J.; He, H. J.; Xu, Q. Q.; Wang, H. O.; Yin, C. H.; Liu, L. Q. *Front. Environ. Sci. Eng.* **2011**, *5*, 402−408.

(48) Jones, C. W. *Annu. Rev. Chem. Biomol. Eng.* **2011**, *2*, 31−53.

(49) Chaikittisilp, W.; Khunsupat, R.; Chen, T. T.; Jones, C. W. *Ind. Eng. Chem. Res.* **2011**, *50*, 14203−14210.

(50) Chaikittisilp, W.; Kim, H. J.; Jones, C. W. *Energy Fuels* **2011**, *25*, 5528−5537.

(51) Choi, S. H.; Gray, M. L.; Jones, C. W. *ChemSusChem* **2011**, *4*, 628−635.

(52) Choi, S.; Drese, J. H.; Eisenberger, P. M.; Jones, C. W. *Environ. Sci. Technol.* **2011**, *45*, 2420−2427.

(53) Choi, S. H.; Watanabe, T.; Bae, T. H.; Sholl, D. S.; Jones, C. W. *J. Phys. Chem. Lett.* **2012**, *3*, 1136−1141.

(54) McDonald, T. M.; Lee, W. R.; Mason, J. A.; Wiers, B. M.; Hong, C. S.; Long, J. R. *J. Am. Chem. Soc.* **2012**, *134*, 7056−7065.

(55) Witoon, T.; Chareonpanich, M. *Mater. Lett.* **2012**, *81*, 181−184.

(56) Xu, X. C.; Song, C. S.; Andrésen, J. M.; Miller, B. G.; Scaroni, A. W. *Microporous Mesoporous Mater.* **2003**, *62*, 29−45.

(57) Qi, G. G.; Wang, Y. B.; Estevez, L.; Duan, X. N.; Anako, N.; Park, A. A.; Li, W.; Jones, C. W.; Giannelis, E. P. *Energy Environ. Sci.* **2011**, *4*, 444−452.

(58) Yan, X. L.; Zhang, L.; Zhang, Y.; Qiao, K.; Yan, Z. F.; Komarneni, S. *Chem. Eng. J.* **2011**, *168*, 918−924.